BAOMS Student Bursary Project

FLUORESCENCE IMAGE GUIDED SURGERY: DEVELOPMENT OF A TISSUE PHANTOM MODEL TO INVESTIGATE INFRARED TISSUE PENETRATION OF INDOCYANINE GREEN NANOCOLLOID

Dewi N. Byrne

Abstract

Image-guided surgery is used across a number of surgical specialties and has undergone rapid development in recent years. Within head and neck oncology, real-time optical image guided techniques that use fluorescent dyes have facilitated a minimally invasive approach to sentinel lymph node biopsy. This aids the accurate detection of cervical node micrometastases and reduces the need for elective neck dissections in the radiographically N0 neck. Traditional blue dyes provide suboptimal fluorescent properties leading to limited tissue penetration and poor retention within the node. More recently, fluorescent nanoparticle dyes, including indocyanine green (ICG) nanocolloid, offer superior properties and have been developed to enhance image acquisition for more reliable sentinel lymph node detection in combination with nuclear tracer techniques.

This study investigated the properties of ICG-nanocolloid by developing a laboratory porcine tissue phantom model. Using this model, the study aims to evaluate the effectiveness of a custom built near-infrared camera – the 'Clinical Spectral Imager' (CSI)– used in sentinel lymph node biopsy in early oral cancer. Secondary aims were to determine the depth of tissue penetration of indocyanine green, ICG nanocolloid and thermocycled ICG nanocolloid and to test the hypothesis that thermocycling of ICG nanocolloid improves fluorescent properties, resulting in increased brightness and greater tissue penetration.

The CSI proved to be effective at detecting dye through porcine tissue. Results showed a concentration dependent fluorescent response. Tissue depth penetration was observed to be in excess of 10 mm, but no significant difference ($p>0.05$) was found in the fluorescent signal between different dye types.

Key words*:*
image-guided surgery, near infrared, indocyanine green, fluorescent nanoparticle, sentinel lymph node biopsy, imaging phantom

Introduction

Intraoperative optical image guidance using coloured dyes assists surgeons by exploiting the properties of light and its effects on tissue characteristics. This offers a number of distinct advantages, including delineation of anatomical structures and pathological tissue, and real time visual feedback to the operating surgeon.

Blue dyes have formed the initial standard for intraoperative image guidance, frequently used in sentinel lymph node (SLN) biopsy procedures with to facilitate detection of nodal micrometastases, offering accurate tumour staging and a reduction in surgical morbidity.[1] However, conventional dyes that utilise light in the visible spectrum (400 – 600 nm) such as methylene blue can hinder the view of the surgical field, and have limited depth penetration through tissue.[2] The near infrared (NIR) fluorescent dye indocyanine green (ICG) provides an alternative. ICG imaging gives a crucial advantage over optical imaging in the visible light range – within the NIR range of 650 – 900 nm the absorption coefficient of tissue is minimal, allowing for much improved depth penetration of light.[3] With the assistance of an infrared camera, the surgeon can therefore view deeper structures.

Optical imaging using ICG has been trialled successfully in feasibility studies for SLN mapping in breast cancer, melanoma and gastric cancer.[4-6] Performing biopsy can prevent the need for full lymph node dissection resulting in less aggressive surgery and reduced morbidity with the same oncological outcome.[7] Within head and neck cancer, SLN biopsy is yet to be considered the gold standard approach. However evidence suggests it to be an effective diagnostic technique. A meta-analysis of studies investigating squamous cell carcinoma of the oral cavity, oropharynx, hypopharynx and larynx showed that all SLN biopsies performed in the included studies correlated with results of subsequent neck dissection - a negative predictive value of 100%.[8]

Intraoperative optical image guidance is currently being investigated in patients with early oral squamous cell carcinoma, with on-going work evaluating the utility of a hybrid fluorescent and radioisotope nanoparticle tracer in identifying the sentinel lymph node and occult metastases in patients with radiologically N0 necks.[9] The combined fluorescent and nuclear detection aims to give enhanced target localisation by allowing improved sensitivity and detection of small and deeply localised lesions.[10] The tracer, indocyanine green technetium-99m albumin nanocolloid (ICG-99mTc-Nanocoll) is detected by use of a gamma camera for the radioisotope component, and a separate NIR camera – the clinical spectral imager (CSI) – for the fluorescent component. This hybrid approach aims to enhance the detection of the sentinel node and reduce the chance of false-negative node sampling.[9] The CSI is a one-of-a-kind, custom-built device that has not undergone testing to determine NIR detection characteristics. It is not known how reliably fluorescent tracers are detected by the camera, or the tissue depth of detection.

There are further concerns that the fluorescent component of the tracer (ICG-nanocoll) may not be bright enough for optimal clinical detection through tissue layers. Attempts have been made to improve the fluorescent yield through the process of thermocycling – repeated heating and cooling within the laboratory of a mixture of dye and protein component of the tracer. Initial investigations have suggested that thermocycling could prove effective in improving fluorescent properties,[11] thus allowing more reliable and effective sentinel lymph node identification within the operating theatre.

The purpose of this study, therefore, was to develop an ex vivo tissue phantom

model for evaluating the fluorescent characteristics of ICG nanocoll and the effectiveness of the Clinical Spectral Imager in NIR fluorescence detection and its' feasibility for clinical use. Secondary aims were to determine the depth of tissue penetration of ICG nanoparticles, and to test the hypothesis that thermocycling of ICG nanocolloid improves fluorescent properties, resulting in increased brightness and greater tissue penetration.

Materials and methods

Chemicals

- Indocyanine green (ICG-Pulsion, 5mg/ml injection)
- Human Albumin Colloidal Particles (Nanocoll 500ug kit for radiopharmaceutical preparation, GE Healthcare)

Clinical Spectral Imager

For obtaining images a charge-coupled-device (NIR) camera unit - the Clinical Spectral Imager, designed as suitable for operating theatre requirements - was used. The device consists of a widefield imager carrying illumination/excitation light from a control centre. White light and fluorescence images of the same surgical field can be captured, and these images can be viewed separately or combined on a monitor. Sensitivity to the fluorescence signal can be altered by adjustments to the gain and integration.

Nanocoll/ICG preparation

Nanocoll was prepared from powder form as per manufacturer's instructions, and purified using a Microcon Centrifugation Filter Device. Free ICG (F-ICG) solution was prepared by mixing ICG powder with water for injection. Nanocoll and free ICG mixing was carried out. Room temperature ICG nanocolloid (RT-ICG) was prepared by leaving the mixed ICG-nanocoll at room temperature for 30 minutes to allow particle association to take place. A thermocycling process of 10 repeating cycles at 65 ºC for 2 minutes and 4 ºC for 2 minutes was used to prepare thermocycled ICG nanocolloid solution (TC-ICG).

Samples were stored in vials wrapped in foil and refrigerated at 4 ºC until required for use within 24 hours of preparation. Immediately prior to imaging the sample solutions were diluted to the required concentration with water for injection. 300 µl were placed one well of a 96 well dish. Four samples (TC-ICG, RT-ICG, F-ICG and a control of water for injection) were arranged in close proximity in order to fit within the camera field of view for image capture. All images were taken with the transparent cover placed over the dish to avoid contamination from the phantom tissue.

Camera set up

A 96 well assay dish containing the four sample solutions was placed in a specially modified black plastic box to exclude background ambient light. A small opening was made in the lid of the box to allow insertion of the wide field imaging head at a reproducible distance from the specimen of 300 mm. This corresponded to a field of

view of 40 mm x 55 mm. Additional ambient light exclusion was achieved by the use of black tape and a black cloth drape to block any small gaps.

The excitation and emission wavelengths on the imager were set to the optimal fluorescence characteristics of ICG at 784 nm and >800 nm respectively. The maximum possible sensitivity to fluorescence signal was achieved by adjusting the control unit settings to gain of x10 and integration time of 4 seconds. Two camera settings were used for image capture – a 'high' setting of gain x10 and integration 0.5 s, and a 'low' setting of gain x1 and integration time of 40 ms.

A white balance was taken with a white surgical swab. Positioning of the specimens and camera was checked using the white light setting, and the image brought into focus. Specimen images were then taken using the fluorescence only setting. Integration time was then reduced to identify the minimum integration setting that a fluorescent signal became visible on the monitor.
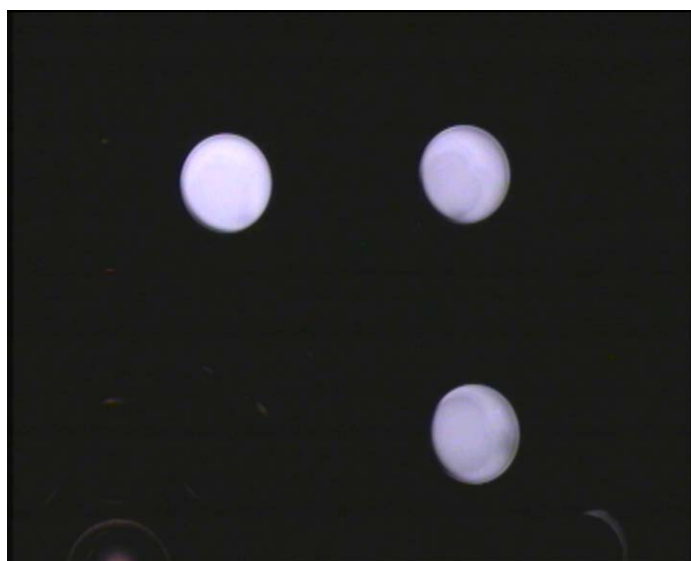
Figure 1. NIR image taken during preliminary testing at ICG concentration 7.5 µM, no phantom. (Clockwise from top left TC-ICG RT-ICG, F-ICG, control)

Phantom tissue preparation

Fresh pork loin joint was purchased in the morning prior to use. Tissue was prepared using a precision slicer (Andrew James UK Ltd) allowing variable cutting thicknesses in 1mm increments from 1 - 15mm. Tissue slices were placed over the cover lid of the prepared dish prior to image capture.

Fluorescence measurement and image brightness quantification

The Clinical Spectral Imager was connected to a laptop via the S-video out of the control unit. An analog to digital convertor USB Video & Audio Grabber (Winstars Technology Ltd), provided S-video to USB 2.0 interface linkage. Digital images were captured using BlazeVideo HDAV Grabber software and stored in bitmap (.BMP) format.

Each bitmap image captured consisted of four regions of interest - one control cell and three fluorescent foci corresponding to F-ICG, RT-ICG and TC-ICG. ImageJ software was used for brightness analysis. Each pixel within an image was assigned a

luminence value from 0 (black) to 255 (white) based on the combined red/green/blue luminence values. The mean pixel luminance value of a representative background area was first determined. The captured image was subdivided into these areas of interest. Each subdivision corresponded with the individual cell of a sample specimen and the immediate dark surrounding area. For all subdivisions, the fluorescent area was isolated and analysed.

Signal to background ratio (SBR) was calculated by dividing the mean pixel luminance value of the fluorescent focus by the background mean, to give a value in arbitrary units.

Six repetitions were undertaken with newly prepared chemicals on each occasion.

Data analysis

Statistical analyses were carried out in Stata statistical software (StataCorp, 2009). Statistical significance was set at 5% (p>0.05)

Results

Dye concentration

Figures a and b demonstrate the effects of different dye concentrations on SBR. A trend of a concentration dependent response was observed – with increasing concentration there was an increase in the calculated SBR. This increase was observed to plateau and possibly decrease at 10 µM – 25 µM. An exception to this pattern was observed on a high camera setting with no tissue penetration (figure a), where SBR peaked at a concentration of 1 µM before markedly decreasing at higher concentration levels. A concentration dependent response is observed at each tissue depth.

Analysis using a generalised linear model revealed a statistically significant effect on SBR for dye concentrations 1.0 µM (p = 0.045), 5.0 µM (p = 0.001), 10.0 µM (p=0.000), 25.0 µM (p=0.000), 50.0 µM (p=0.000).

ICG dye type

Analysis using a generalised linear model showed there was no detectable main effect for any one of the three dye types (p>0.367). Figure c shows a possible trend towards higher SBR with TC-ICG, however this was not statistically significant.
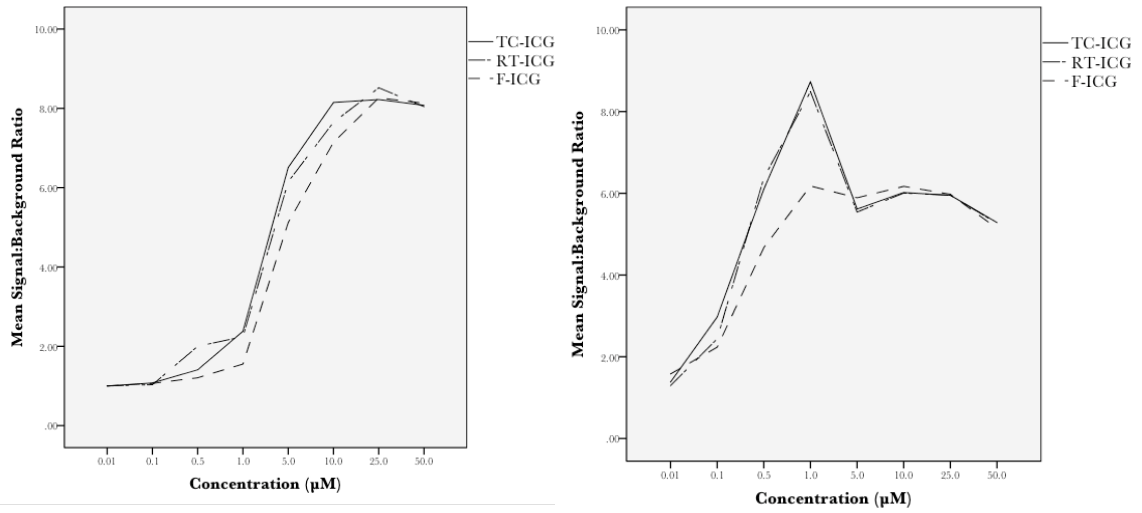
Figure a. Graphs to show signal to background ratio concentration-dependent response to TC-ICG, RT-ICG, F-ICG. Each data point is the mean of six replicates. Low camera setting (left) and high camera setting (right)
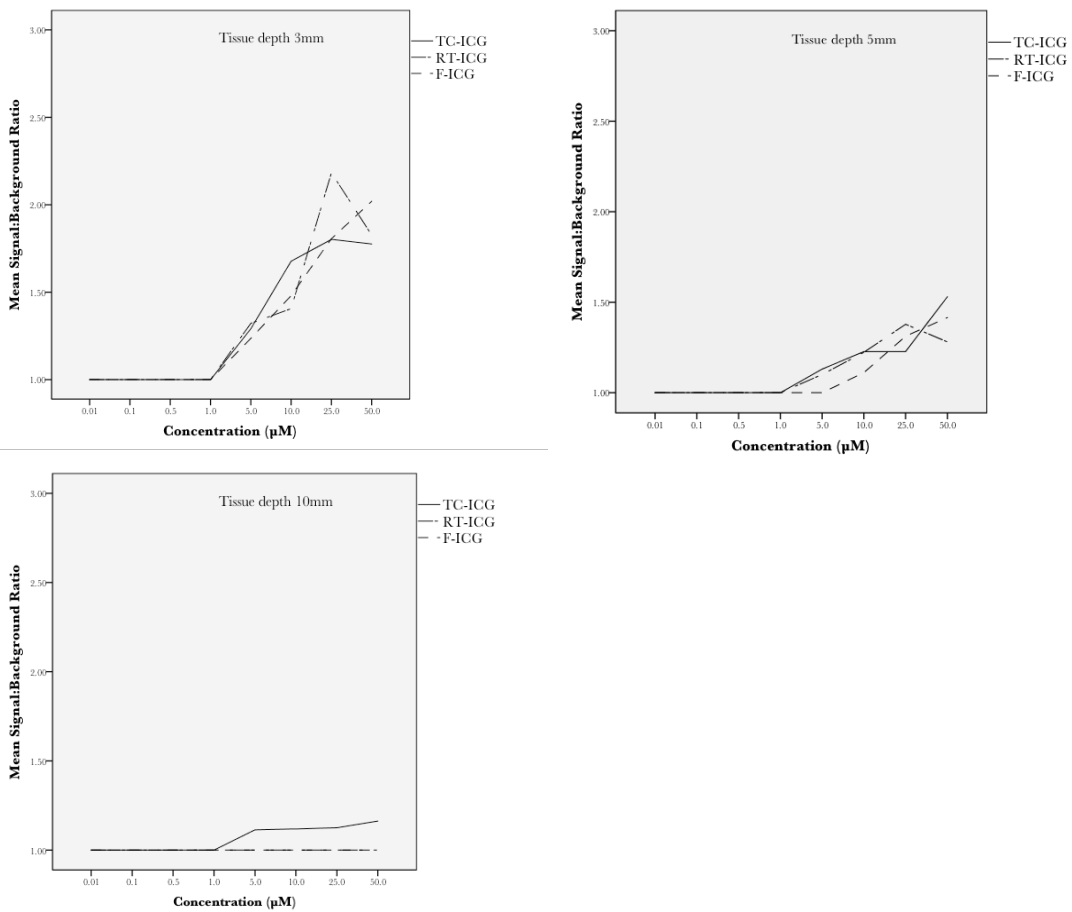

Figure b. Graphs to show signal to background ratio concentration-dependent response to TC-ICG, RT-ICG, F-ICG, at tissue depths of 3 mm, 5 mm and 10 mm. Low camera setting. Each data point is the mean of six replicates.
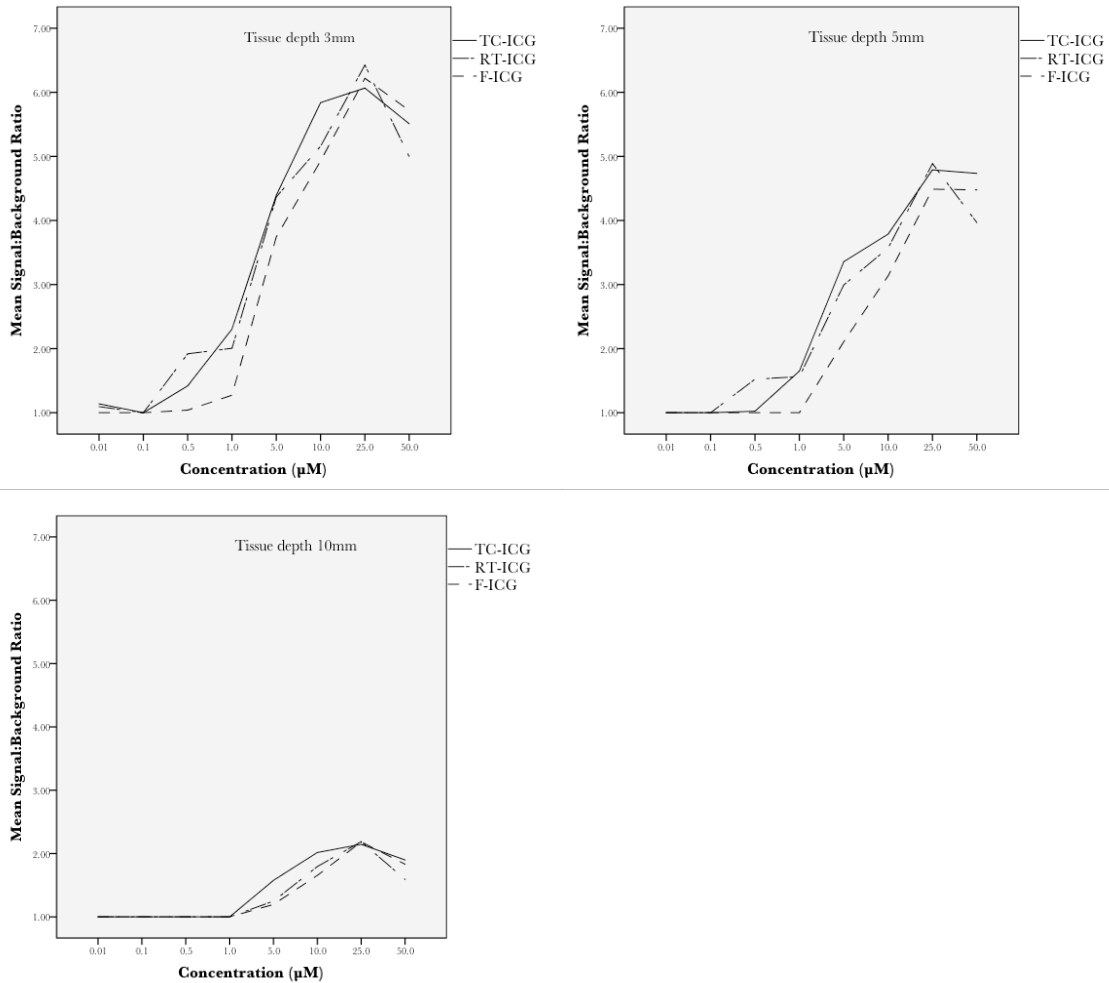
Figure c. Graphs to show signal to background ratio concentration-dependent response to TC-ICG, RT-ICG, F-ICG, at tissue depths of 3mm, 5mm and 10mm. High camera setting. Each data point is the mean of six replicates.

Tissue depth

There was a reduction in SBR with increasing tissue depth. Analysis using a generalised linear model showed a statistically significant SBR difference between 0 mm and 3 mm (mean difference 2.44, 95% CI 2.03 to 2.83), 3 mm and 5 mm (mean difference 0.51, 95% CI 0.11 to 0.91) and 5 mm to 10mm (mean difference 0.61, 95% CI 0.21 to 1.01). At low camera settings, complete loss of signal was observed at a tissue depth of 10 mm, with the exception of TC-ICG at concentrations greater than 1 µM. At high camera settings, signal was observed for all three dyes at concentrations greater than 1 µM.
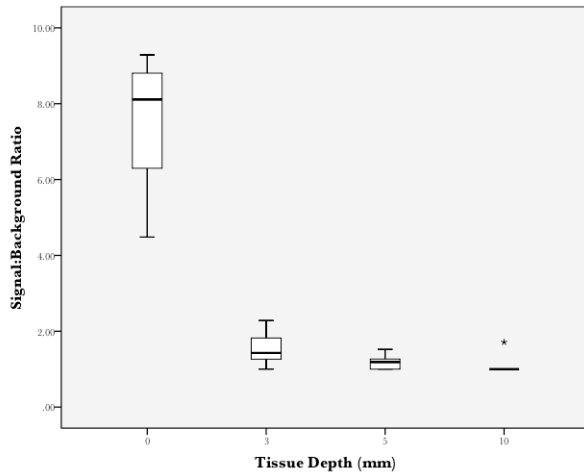
Figure d. Boxplot of effect of tissue depth on signal to background ratio (median, range and interquartile range) at dye concentration 10 μM, low camera setting.
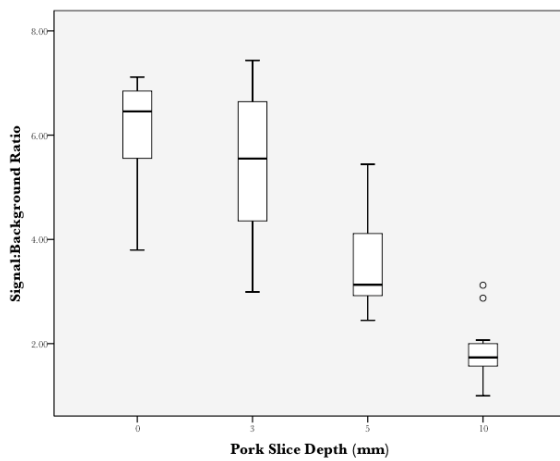
Figure e. Boxplot of effect of tissue depth on signal to background ratio (median, range and interquartile range) at dye concentration 10 μM, high camera setting.

Discussion

The tissue phantom model that has been developed provides a simple and effective system for investigating CSI imaging system and ICG nanocolloid. Independent variables (concentration, dye preparation, tissue depth) can be easily and accurately manipulated within a controlled environment.

Results show the imaging system is able to effectively identify three different preparations of ICG nanocolloid, at different concentrations beneath varying depth of muscle tissue. Through software manipulation, the fluorescent brightness of those images produced can be quantified. Camera setting adjustment can easily facilitate optimal image acquisition, with higher gain and integration settings more readily able to detect weaker fluorescent signals. The potential feasibility for clinical application is clear, although further work is required in order to apply the principles of software interpretation outlined in this study to the operating theatre.

From a practical perspective, the CSI can be positioned on a small trolley, which affords good portability. A flexible gooseneck arm carrying the camera head

can be fixed to the trolley or operating table, permitting alterations in height and angle over the surgical field.

As predicted, increasing the depth of tissue acted to reduce the detected fluorescent signal. Changes in SBR with increasing tissue depth can be attributed to the effects of scattering and absorbance of NIR light as photons penetrate biological tissues.[3] At low camera settings, 10mm of tissue depth did not permit penetration of fluorescent signal for the RT-ICG and F-ICG, with a weak signal observed for TC-ICG at concentrations of greater than 1 µM. However, at high camera settings, a weak signal was observed for all three dyes at concentrations greater 1 µM. The maximum depth penetration has not been determined and is greater than 10 mm, but given the low SBR at this level, the maximum practicable depth is unlikely to be significantly higher.

These results are comparable with prior studies that have looked into fluorescent tissue penetration. Within the laboratory setting Chernomordik et al.[12] showed accurate visualisation, size estimation and 3D localisation using fluorescent latex dyes up to a maximum depth of 12 mm. An ex-vivo porcine tissue phantom, comparable to the present investigation, was utilised. This 12 mm depth penetration is in excess of our 10 mm findings for ICG nanocoll. However, NIR camera acquisition and integration times were greater, varying from 1 s at 4 mm depth testing, to 8 s at 12 mm. These integration times were possible since static imaging was undertaken, without consideration of image distortion created by camera movement. The CSI – designed for mobility and portability within the operating theatre – does not afford this luxury, and hence a maximum integration of 0.5 s was necessary.

Quan et al.[13] found still further pork muscle depth penetration when investigating ICG silica nanoparticles. Good penetration was seen to a depth of 20 mm. This increased depth is likely as a result of enhanced fluorescent properties of the silica nanoparticles, in combination with a higher camera integration time of 5 s.

Limitations

Statistical analysis of results showed a high degree of data variability, with relatively few replicates. This represents limitations to the design and application of the study. Possible sources of error include sample contamination with dust particles, incomplete exclusion of ambient light, inconsistencies in the depth of pork and a failure to take account for the autofluorescent properties of the phantom tissue. Further work is needed to refine the study protocol to account for these sources of error.

The phantom study protocol suffers from oversimplification of a process that is more complex when applied to a human subject. Within the operating theatre, further factors of route of administration, pharmacokinetics and lymphatic distribution must be considered in addition to dye concentration and depth of penetration. Following peritumoural injection, ICG nanocoll particles pass through the lymphatic vessels to the lymph node, where they are trapped within reticular cells and accumulation allows for detection with the NIR camera. At the injection site some of the remaining tracer is phagocytosed into local histiocytes passing into the circulating blood before being broken down via the reticuloendothelial system or excreted by the kidneys.[3] Studies looking at intraoperative imaging in mouse models for metastatic breast and prostate cancer[14] have shown nanocolloid has a favourable particle size for SLN accumulation and subsequent imaging, however, the recognition of dye particles

by the immune system may also play an important role in the accumulation of tracer in the SLN[15] and further work is needed in this area.

Conclusion

The results have provided s useful preliminary information on the CSI's effectiveness and the ICG-nanocoll fluorescent penetration of tissue. On-going clinical research using the CSI is being undertaken to assess the additional benefit of the ICG fluorescent probe during sentinel lymph node biopsy in oral cancer, when compared with gamma tracer detection alone.

References

1. Morton DL, Wen DR, Wong JH, Economou JS, Cagle LA, Storm FK, et al. Technical details of intraoperative lymphatic mapping for early stage melanoma. Arch Surg. 1992 Apr;127(4):392–9.

2. Keereweer S, Kerrebijn JDF, Driel PBAA van, Xie B, Kaijzel EL, Snoeks TJA, et al. Optical Image-guided Surgery—Where Do We Stand? Mol Imaging Biol. 2010 Jul 9;13(2):199–207.

3. te Velde EA, Veerman T, Subramaniam V, Ruers T. The use of fluorescent dyes and probes in surgical oncology. European Journal of Surgical Oncology. 2010 Jan 1;36(1):6–15.

4. Troyan SL, Kianzad V, Gibbs-Strauss SL, Gioux S, Matsui A, Oketokoun R, et al. The FLARE intraoperative near-infrared fluorescence imaging system: a first-in-human clinical trial in breast cancer sentinel lymph node mapping. Ann Surg Oncol. 2009 Oct;16(10):2943–52.

5. Symeonidis D, Koukoulis G, Tepetes K. Sentinel node navigation surgery in gastric cancer: Current status. World J Gastrointest Surg. 2014 Jun 27;6(6):88–93.

6. van der Vorst J r., Schaafsma B e., Verbeek F p. r., Swijnenburg R j., Hutteman M, Liefers G j., et al. Dose optimization for near-infrared fluorescence sentinel lymph node mapping in patients with melanoma. British Journal of Dermatology. 2013 Jan 1;168(1):93–8.

7. Yi M, Giordano SH, Meric-Bernstam F, Mittendorf EA, Kuerer HM, Hwang RF, et al. Trends in and outcomes from sentinel lymph node biopsy (SLNB) alone vs. SLNB with axillary lymph node dissection for node-positive breast cancer patients: experience from the SEER database. Ann Surg Oncol. 2010 Oct;17 Suppl 3:343–51.

8. Thompson CF, St John MA, Lawson G, Grogan T, Elashoff D, Mendelsohn AH. Diagnostic value of sentinel lymph node biopsy in head and neck cancer: a meta-analysis. European Archives of Oto-Rhino-Laryngology. 2013 Jul;270(7):2115–22.

9. Schilling C, Corrado A, Gnanasegaran G, McGurk M. Role of intraoperative sentinel node imaging in head and neck cancer. Clin Transl Imaging. 2015 Apr 18;3(3):217–23.

10. Holman B, Tumeh SS. Single-photon emission computed tomography (spect): Applications and potential. JAMA. 1990 Jan 26;263(4):561–4.

11. Stepan Koudelka, 2015, personal communication.

12. Chernomordik V, Gandjbakhche A, Smith P, Russo A. Three-dimensional localization of fluorescent masses deeply embedded in tissue. Physics in Medicine & Biology. 2002 Nov;47(22):4079–92.

13. Quan B, Choi K, Kim Y-H, Kang KW, Chung DS. Near infrared dye indocyanine green doped silica nanoparticles for biological imaging. Talanta. 2012 Sep 15;99:387–93.

14. Ravizzini G, Turkbey B, Barrett T, Kobayashi H, Choyke PL. Nanoparticles in sentinel lymph node mapping. WIREs: Nanmed Nanobiotech. 2009 Nov 1;1(6):610–23.

15. Argon AM, Duygun U, Acar E, Daglioz G, Yenjay L, Zekioglu O, et al. The Use of Periareolar Intradermal Tc-99m Tin Colloid and Peritumoral Intraparenchymal Isosulfan Blue Dye Injections for Determination of the Sentinel Lymph Node: Clinical Nuclear Medicine. 2006 Dec;31(12):795–800.